Use of Generalized N-dimensional Lissajous Figures for Phase Retrieval from Sequences of Interferometric Images with Unknown Phase Shifts

Armando Albertazzi, Analucia V. Fantin, Allison F. Maia,
Daniel P. Willemann, Mauro E. Benedet, and Matias Viotti

Mechanical Engineering Department, Universidade Federal de Santa Catarina,
Florianópolis, Brazil
albertazzi@labmetro.ufsc.br

1 Introduction

There are several engineering applications for interferometry where the measurement must be done in-situ in presence of mechanical vibrations or other disturbances. In those cases, optical techniques based in a single image acquisition are the best choices. Approaches like pixelated phase-mask interferometers, instantaneous or simultaneous phase measuring interferometry have been successfully reported in the literature. However, some of them are quite complex or difficult to be miniaturized or made robust enough to be transported and operated in quite hostile environments.

In those cases where it is not possible to use simultaneous interferometers, compact temporal phase shifting interferometers, operating with short light pulses, could be good choices. A set of interferometric images must be sequentially acquired with predefined phase shifts. However, the presence of disturbances, mainly vibrations, can introduce unknown phase deviations resulting in a sequence of images with unknown phase shifts. The literature presents few approaches for retrieving phase information from sequence of images with unknown phase shifts using optimization methods [1], [2], [3]. This paper presents a quite different approach using Lissajous figures. To improve the robustness of the approach, the authors introduce the concept of generalized *N-dimensional Lissajous figures*.

2 Lissajous Figures

Lissajous figures are a family of parametric 2D curves frequently used to establish the frequency ratio or relative phase between two harmonic signals. They were initially investigated by Nathaniel Bowditch in 1815, and later in more detail by Jules Antoine Lissajous in 1857. Figure 1 presents four examples for harmonic

W. Osten (ed.), *Fringe 2013*,
DOI: 10.1007/978-3-642-36359-7_26,

signals with different frequency ratios. To obtain a Lissajous figure, one harmonic signal is plotted along the X axis and the other signal along the Y axis. Every time the frequency ratio is a rational fraction (formed by integer numbers), a closed and stable figure is obtained.

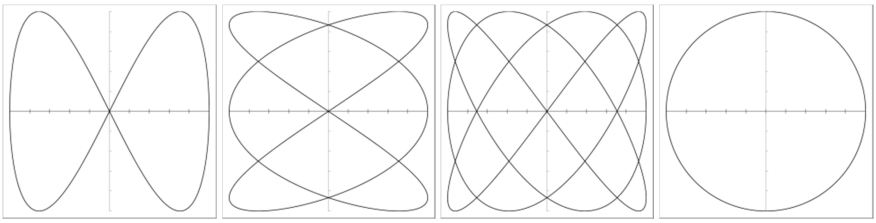

Fig. 1 Examples of Lissajous figures for frequency ratios f_Y/f_X of 1/2, 3/2, 3/4 and 1/1 respectively

If the frequencies of both signals are the same, the resulting Lissajous figure is an ellipsis. If the amplitudes are equal and the phase difference is ± 90°the ellipses become a circle. The effect of phase difference on both signals is demonstrated in figure 2. If the phase difference is 0° the ellipses degenerates to a +45° straight line. If the phase difference is 180° the ellipses becomes a -45° straight line.

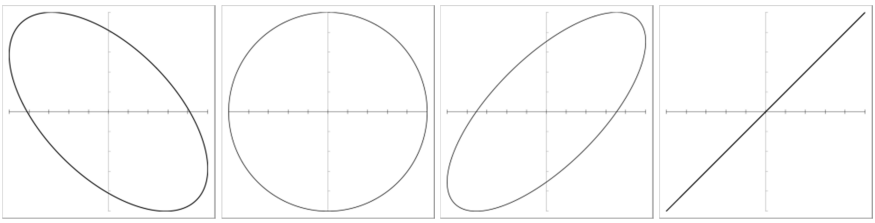

Fig. 2 Effect of different phase values (125°, 90°, 45°, 0°) in a 1/1 ration Lissajous figure

3 Phase Determination from Lissajous Figures

If the light intensities of two different points of an interferogram are plotted in the X and Y axis while the phase of the interferogram is continuously shifted, a Lissajous ellipsis is progressively drawn. The shifted phase value is the parametric variable. Initially consider a particular case where the two points have 90° phase difference and the same amplitude in such a way that the Lissajous figure is a perfect circle. When a phase shift $\Delta\theta$ is applied to the interferogram, it produces a rotation of the same amount in a vector with origin at the circle center and end at the circle line. If $\Delta\theta$ is unknown it can be determined from the observed vector rotation on the Lissajous figure. That is the main idea behind this paper.

In the general case that the phase difference between the two selected points is not 90°, and/or the modulation amplitude is not the same, the Lissajous figure is

an ellipsis. By finding the ellipsis parameters, it is possible to compute the rotation angle as well. The general parametric ellipses equation in polar coordinate are:

$$X(\theta) = X_c + R_1 \cos(\theta)\cos(\varphi) - R_2 \sin(\theta)\, sin(\varphi) \tag{1A}$$

$$Y(\theta) = Y_c + R_1\, cos(\theta)\, sin(\varphi) + R_2\, sin(\theta)\, cos(\varphi) \tag{1B}$$

where X_C and Y_C are the ellipsis center coordinates, R_1 and R_2 are the principal radius values, φ is the angle between the principal axes of the ellipsis and the X axes, and θ is the polar angle. Fitting an ellipsis by the least squares method is not a trivial task. A very efficient and robust approach using eigenvalues and eigenvectors can be found in [4]. Once the ellipse parameters are determined, the polar angle θ_0 of a given point (x_0, y_0) on the ellipses line can be computed by:

$$\tan(\theta_0) = \frac{R_1}{R_2} \frac{(y_0 - Y_C)\cos(\varphi) - (x_0 - X_C)\sin(\varphi)}{(y_0 - Y_C)\sin(\varphi) + (x_0 - X_C)\, cos(\varphi)} \tag{2}$$

If a set of five or more discrete images with unknown and different phase shifts are acquired, the ellipsis equation can be fully determined and the discrete points used to calculate the relative phase shifts. Although this approach is mathematically correct, it is not very robust in the presence of random errors. It is not also possible to guarantee that the resulting ellipsis will not degenerate to a straight line, or be closed to it, enlarging significantly the uncertainties on angle determination.

4 Generalized N-dimensional Lissajous Figures

To improve the robustness of the approach, the authors introduce the concept of generalized N-dimensional Lissajous figures. Instead of using only the *XY* plane, additional dimensions can be added. For example, if the light intensity of a third point in the interferogram is now associated with the Z axis, a 3D Lissajous figure is constructed. The resulting ellipsis is no longer in the *XY* plane. However, it can be verified that it remains a plane line, i.e., it lies in an oblique 2D plane in space. If N points are taken, an N-dimensional Lissajous figure is obtained. Also in this case, the resulting figure still remains an ellipsis and that lies in a 2D plane.

The 2D projection of the N-dimensional ellipsis can also be used to compute the unknown phase shifts from the sequence of interferograms. The resulting estimation is less sensitive to noise since it uses a much larger amount of data. The chance of the ellipsis degenerates to a straight line becomes smaller as the number of dimensions increase.

The 2D projection coordinates of the N-dimensional ellipses can be computed using two orthogonal vectors that lie in the ellipsis plane. They can be formed from two vectors connecting two different pairs of points on the ellipses. Since the 2D coordinates are available, the ellipsis equation is determined by least square fitting and the phase angle is determined for each interferogram by equation (2).

5 Phase Calculation from Irregularly Phase Shifted Images

Once the phase shifts are determined for each interferogram image from the *N*-dimensional Lissajous figure, the phase value can be determined for all remaining points of the images. A phase calculation equation for *K* irregular phase shifts is also presented in this paper.

Let's $I_i(x, y)$ be the intensity distribution of the *i-th* interferogram, where $i = 1$ to *K*. Let's also assume that all the phase shift value θ_i were previously determined for each *i-th* image from the N-dimensional Lissajous figures. The phase values $\gamma(x, y)$ for each pixel (x, y) of the image can be determined from equation (3). The coordinates (x, y) where suppressed for compactness.

$$\tan(\gamma) = -\frac{(K.SIS - SS.SI)(SC^2 - K.SCC) + (K.SIC - SC.SI)(K.SSC - SC.SS)}{(K.SIS - SS.SI)(K.SSC - SC.SS) + (K.SIC - SC.SI)(SS^2 - K.SSS)} \tag{3}$$

The quantities on equation (3) are computed from image intensities $I_i(x, y)$ and phase shift value θ_i as follows. All the summations are ranging from $i = 1$ to *K*:

$$SI = \sum I_i(x, y) \qquad SSC = \sum[\cos(\theta_i)\sin(\theta_i)]$$
$$SC = \sum \cos(\theta_i) \qquad SS = \sum \sin(\theta_i)$$
$$SIC = \sum[I_i(x, y)\cos(\theta_i)] \qquad SIS = \sum[I_i(x, y)\sin(\theta_i)]$$
$$SCC = \sum \cos^2(\theta_i) \qquad SSS = \sum \sin^2(\theta_i)$$

6 Application Example

An application example is given using a sequence of phase shifted images obtained from shearography. A protective layer of composite material applied over a steel surface was tested for adhesion defects. The surface was heated-up by about 10°C and it was analyzed while it was cooling down. An ideal phase shift of 90° was applied by a piezo translator (PZT) before a new image was acquired. However, due to thermal currents, and PZT non-linearity, and other instabilities, the resulting phase shifts were note accurately known. Therefore, no previous assumption on the phase shifts values was used at all.

A region of interest was defined over an area where high gradient deformations where not expected. A set of $K = 8$ initial images was analyzed by a software that implements the developed approach. A total number of $N = 300$ points were selected inside the region of interest based on their maximum intensity fluctuation. The 300-dimensional ellipsis was computed and analyzed. Figure 3(b) shows the resulting projected ellipsis. Each point on the ellipses corresponds to a different interferogram. The relative phase shifting among the interferograms can be computed after least square fitting of the ellipsis and using equation (2). It can be clearly noted in Figure 3 that the real phase shifts were not accurately equal to 90° as ideally it supposes to be. The phase value was computed for each image pixel using the computed phase shifts and equation (3). The data processing time is almost instantaneous.

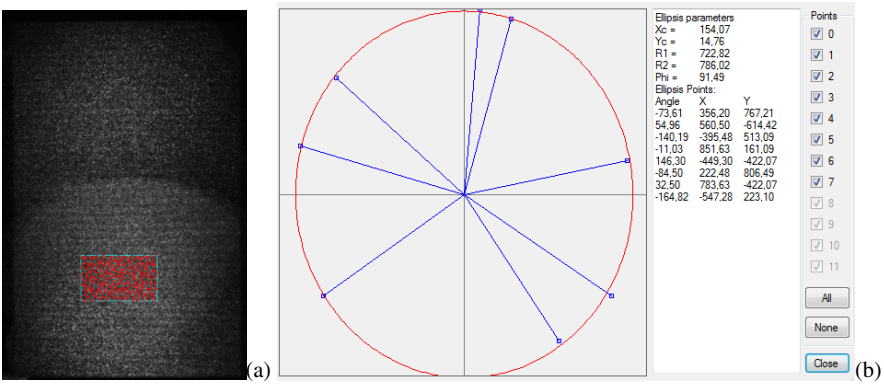

Fig. 3 (a) Shearography image and the defined region of interest with 300 points used to compute the phase increments; (b) 2D projection of the N-dimensional ellipses from a set of eight shearography images with unknown phase shifts

Another set of $K = 8$ images was acquired after the test surface had cooled down. The same procedure was repeated, so another ellipsis was obtained and the phase shifts determined. Also here, the phase value for each image pixel was computed from equation (3). Finally the wrapped phase differences were computed for each image pixel. They are shown in Figure 4. Note the high image quality obtained from two sets of non-stable images with unknown phase shifts.

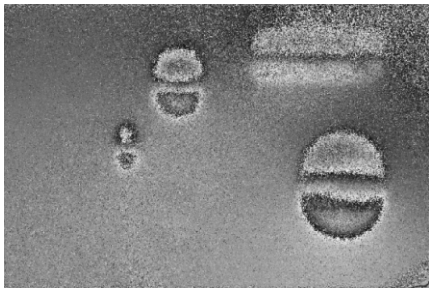

Fig. 4 Wrapped phase difference from two sequences of shearography images with unknown phase shifts

7 Conclusions

This paper presents an alternative approach to compute phase values from a set of five or more unknown phase shifted images. The approach combines data from several good modulation points on the image to form an N-dimensional Lissajous

ellipsis. An overall phase shift value is determined from the fitted ellipsis for each interferogram. Finally, the phase shifted values are used to determine the phase value for each image pixel.

The method itself is potentially robust since it uses a large amount of data from each interferogram, reducing the influence of noise and the chances of ill-conditioning. The computational effort to compute the arbitrary phase shifts is virtually negligible. A generalized equation for phase calculation from non-uniform phase shifts is also presented.

The application example in a set of unknown phase shifted images obtained from a shearography test shows very good quality phase difference maps.

The authors are currently analyzing the behavior of the algorithm more deeply and exploring its applications to pulsed shearography in highly vibrating environments.

Acknowledgments. The authors would like to thanks PETROBRAS and IBP for technical and financial support for this work through SHIC project.

References

1. Okada, K., Sato, A., Tsujiuchi, J.: Simultaneous calculation of phase distribution and scanning phase shift in phase shifting interferometry. Optics Communications 84, 118–124 (1991)
2. Wang, Z., Han, B.: Advanced iterative algorithm for phase extraction of randomly phase-shifted interferograms. Optics Letters 29, 1671–1673 (2004)
3. Hildebrand, A., Falldorf, C., von Kopylowa, C., Bergmann, R.B.: A fast and robust approach to phase shift registration from randomly phase shifted interferograms. In: Doval, Á.F., Trillo, C., López-Vázquez, J.C. (eds.) Speckle 2012: V International Conference on Speckle Metrology. Proc. of SPIE, vol. 8413, p. 84130R (2012)
4. Fitzgibbon, A., Pilu, M., Fisher, R.B.: Direct Least Square Fitting of Ellipses. Patern Analysis and Machine Intelligence 21(5) (May 1999)